Chemical Engineering Journal 155 (2009) 829–837

Contents lists available at ScienceDirect

Chemical Engineering Journal

journal homepage: www.elsevier.com/locate/cej

A one-step conversion of benzene to phenol using MEMS-based Pd membrane microreactors

Shu-Ying Ye[a,*], Satoshi Hamakawa[a,**], Shuji Tanaka[b], Koichi Sato[a], Masayoshi Esashi[b], Fujio Mizukami[a]

[a] Research Center for Compact Chemical Process, National Institute of Advanced Industrial Science and Technology (AIST), 4-2-1, Nigatake, Miyagino-ku, Sendai 983-8511, Japan
[b] Department of Nanomechanics, Tohoku University, 6-6-01 Aza Aoba, Aramaki, Aoba-ku, Sendai 980-8579, Japan

ARTICLE INFO

Article history:
Received 16 April 2009
Received in revised form 31 August 2009
Accepted 4 September 2009

Keywords:
MEMS (micro-electro-mechanical system)
Microreactor
Pd membrane
Hydrogen permeation
Direct hydroxylation
Benzene
Phenol

ABSTRACT

We have developed an MEMS-based Pd membrane microreactor for one-step conversion of benzene to phenol, and also evaluated the H_2 permeation characteristics through the Pd membrane before the benzene hydroxylation experiments. The conversion of benzene, selectivity and yield of phenol were investigated by varying the operation conditions. The phenol yield of 20% and benzene conversion of 54% were obtained at a reaction temperature of 200 °C. The phenol and dihydric phenols dominated the distribution of products and the hydrogenation products of from benzene and phenol were absent in the MEMS-based Pd membrane microreactor, which was very different from the macrotubular Pd membrane reactors. The effect of H_2/O_2 ratio on products distribution has been investigated. From the comparison of reaction results with a macrotubular Pd membrane reactor, it is figured out that the Pd membrane microreactors fabricated by MEMS technology gave a higher reaction conversion and product yield.

1. Introduction

Phenol is an extremely important chemical in industry, which is widely used in the production of drugs, dyestuffs and synthetic resin. Phenol is primarily produced by the cumene process, in which benzene is converted via cumene to cumene hydroperoxide. This multi-step process accompanies high-energy consumption and a large amount of acetone as a by-product. To overcome these problems, direct hydroxylation of benzene to phenol using oxidant such as H_2O_2 and N_2O has been studied [1–8]. These oxidants are, however, too much expensive to apply to the commercial production.

The direct hydroxylation of benzene using mixture of O_2 and H_2 is another alternative and has been widely studied in the liquid and gas phase [9–12]. Benzene oxidation in the gas phase seems to be more practicable for industrial applications [12], because the use of solvents is avoided. Although a very high selectivity of phenol (>90%) had been reported by some researchers [12, and references there], the conversion of benzene was less than 2% and resulted that the yield of phenol was also less than 2%. Such a yield of phenol is inadequate for practical use. In addition, there is a serious risk of explosion when H_2 mixes with O_2.

Our research group reported that a tubular Pd membrane reactor (PdMR) [13–18], schematically shown in Fig. 1, promoted hydroxylation and hydrogenation. It should be noted that this type of membrane reactor attained the direct conversion of benzene to phenol (yield ~ 20%). Active hydrogen species, which appear onto the surface via the Pd membrane, can easily react with molecules of oxygen and form active species like HO* or HOO* radicals. Thus, the active species attack benzene, and hydroxylation occurs readily to form phenol. This system is quite simple and can eliminate the risk of explosion because the supplies of O_2 and H_2 are physically separated, but the tubular shape of the Pd membrane has some difficulties to stack them for mass production.

The developments of chemical process miniaturization have taken large strides in the past few decades due to the evolution of micro-electro-mechanical system (MEMS) technology. MEMS technology enables us to integrate reactors with other devices such as pressure transducers, flow controllers and temperature control apparatus to form micro-systems capable of analyzing or synthesizing chemicals [19,20]. More importantly, the miniaturizations of chemical reactors to a micro-scale leads to unique characteristics different from conventional macroreactors, such as low-energy consumption, high surface-to-volume ratio, short response times, good reaction controllability, better heat and mass transfer properties and uniform flow and temperature distributions. In fact, a

* Corresponding author. Current affiliation: MEMS CORE Co. Ltd. 3-11-1, Aketori, Izumi-ku, Sendai 981-3206, Japan. Tel.: +81 22 777 8717; fax: +81 22 777 8718.
** Corresponding author. Tel.: +81 22 237 5211; fax: +81 22 237 5226.
E-mail addresses: yeh@mems-core.com (S.-Y. Ye), hamakawa.s@aist.go.jp (S. Hamakawa).

1385-8947/$ – see front matter © 2009 Elsevier B.V. All rights reserved.
doi:10.1016/j.cej.2009.09.007

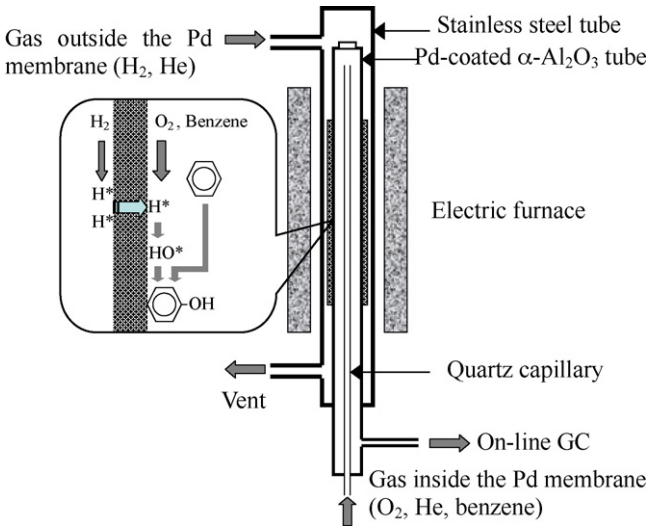

Fig. 1. Tubular PdMR for direct hydroxylation of aromatics and the working principle of the Pd membrane.

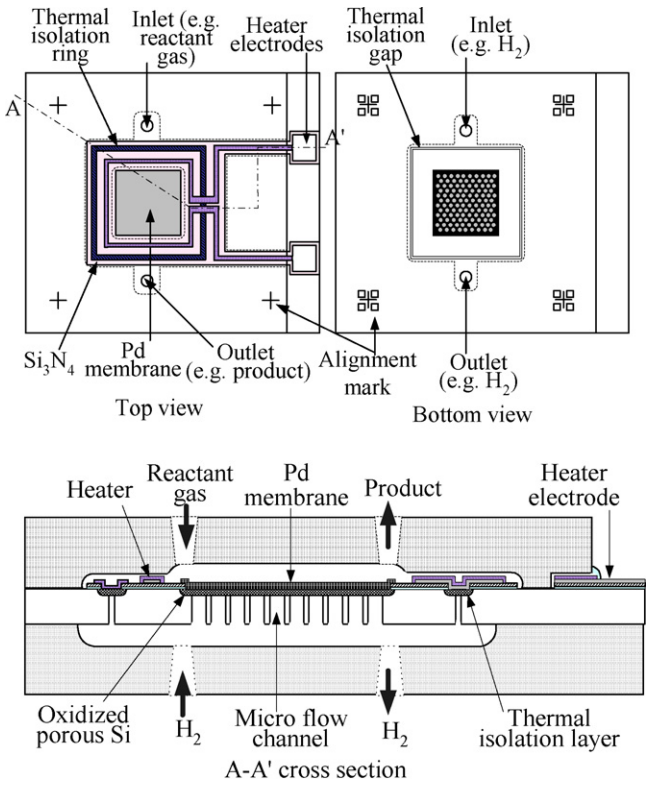

Fig. 2. Structure of MEMS-based PdMMR.

higher conversion and better product yield obtained in microreactors have been observed by some researchers [21–23]. Many fine chemical reactions of interest are constrained by unfavorable thermodynamics that could benefit from the membrane operation. Selective product removal could improve the product purity and achieve supra-equilibrium conversions [21–26]. Miniaturization also enhances the selectivity and permeation of the membrane compared to conventional membrane units [27–28].

We have developed a MEMS-based Pd membrane microreactor (PdMMR) [20] and applied it to the hydrogenation of 1-butene successfully. Since the PdMMR has a micro-dimension, the concentration of reactant gases is almost uniform on the surface of the membrane. Therefore, it is expected that the PdMMR promotes the hydroxylation of the benzene to phenol and increases the yield of phenol. Furthermore, the PdMMR has a possibility of scaling-up laboratory-level experiments directly to commercial production by stacking the same microreactors.

In this study, we demonstrated one-step conversion of benzene to phenol using the MEMS-based PdMMR for the first time. Prior to reaction experiment, we evaluated the gas permeation and permselectivity of the Pd membrane. The conversion, selectivity and yield of reactions were investigated by varying the operation conditions. Each test reaction was carried out and lasted up to 9 h. Results of reactions were compared with those of the macrotubular PdMRs [13–18].

2. Microreactor fabrication

The schematic structure of the MEMS-based PdMMR is shown in Fig. 2. It is composed of three layers: top glass cap, Si substrate and bottom glass cap. H_2 and reaction gas are supplied to the bottom and top side of the Pd membrane, respectively. Reaction products are obtained from the top side. The Pd membrane has a size of 5 mm × 5 mm. Oxidized porous silicon (PS) is served as a structural support for the Pd membrane. Under the oxidized PS support, micro-flow channels with a diameter of 100 μm are opened. A Pt/Ti micro-heater is formed on a Si_3N_4 insulation layer for heating the Pd membrane to improve H_2 permeability and prevent H_2 embrittlement. The oxidized PS ring is also formed around the Pd membrane for thermal isolation. The thermal isolation gap under the oxidized PS ring is 100 μm in width.

The fabrication process of the microreactor is shown in Fig. 3. The microreactor was fabricated from a 300 μm thick ⟨1 0 0⟩ p-type Si wafer polished on the double sides with resistivity of 0.01–0.02 Ω cm. The process started from coating the wafer with a 100-nm thick SiO_2 film and a 300-nm thick Si_3N_4 film by means of wet thermal oxidation and low pressure chemical vapor deposition (LPCVD), respectively. Then, the bilayer film of Si_3N_4/SiO_2, whose stress is compensated, was patterned by standard photolithography, followed by dry CF_4 plasma etching of Si_3N_4 and wet etching of SiO_2 using buffered oxide etch (BOE). In this step, the films of Si_3N_4 and SiO_2 on the backside were also removed.

Within the opened windows of the Si_3N_4/SiO_2 film, PS was formed by anodization in HF-ethanol (C_2H_5OH) electrolyte (HF (50%):C_2H_5OH:H_2O = 1:1:1 in volume). To generate a 30 μm thick PS layer, the anodizing time was 20 min with a current density of 30 mA/cm^2. Furthermore, the PS should be oxidized thermally to stop deep reactive ion etching (DRIE) in the step 7 of the process chart. Next, the Pt/Ti heater was formed around the PS area by sputtering and lift-off process. The ring design of the micro-heater allows a large area of the membrane to be heated. And then, the thermal isolation ring and the heater were covered with SiO_2 to prevent gas from permeating via the thermal isolation ring and to prevent synthesized product from being decomposed by Pt.

The Si substrate was etched from the backside by deep reactive ion etching (DRIE) to release the PS layer and make the flow channels of H_2. After the bottom glass cap was bonded to the Si substrate by anodic bonding technique, a 500-nm thick Pd film was deposited on the surface of the oxidized PS by controlling sputtering time at a substrate temperature of 200 °C. To improve H_2 permeation through the Pd membrane, we did not use any adhesion layer. The final step in the fabrication was to bond the top glass cap to the Si substrate. Both top and bottom cap are made of Pyrex glass and etched in HF (50%) solution to form micro-gas channels. Through holes served as gas inlets and outlets were fabricated by sandblasting from a nozzle. The size of the completed microreactor is 25 mm × 20 mm.

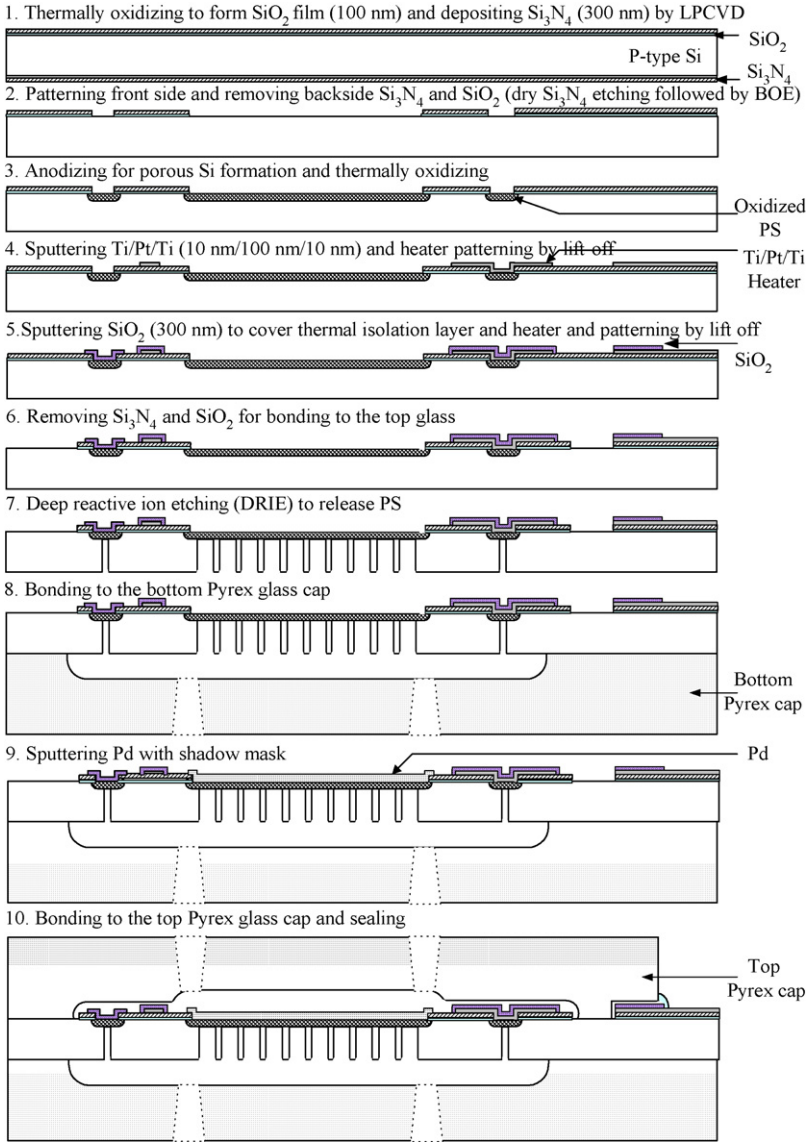

Fig. 3. Fabrication process of MEMS-based PdMMR.

3. Experimental

To achieve the direct hydroxylation of aromatic compounds, a neutral oxygen species or radical oxygen species, such as HO* or HOO*, might work as the active species [29]. It is known that a membrane reactor is an effective tool to produce active oxygen species [30]. In this study, we performed the direct hydroxylation of benzene to phenol using the developed PdMMRs.

The experimental setup is shown in Fig. 4. H_2 was continuously introduced to the lower side of the Pd membrane with the aid of a mass flow controller (MFC). The H_2 pressure was monitored using a pressure transducer. To the other side of the Pd membrane, namely the upper side, a mixture gas of He, N_2, O_2 and benzene was introduced into the PdMMR. In the hydroxylation of benzene, H_2 permeated flux was kept at 1.5 cc/min by adjusting the pressure of H_2 in the inlet during the reaction at 200 °C. Liquid-phase benzene was fed with a syringe pump (Hamilton Company) and the flow rate of benzene was set at 0.08 cc/h. Benzene was vaporized by heating the pipe of the gas inlet. The flow rate of He and N_2 is 2.5 sccm (room temperature and ambient atmosphere). To investigate the effect of ratio of H_2 to O_2 on products distribution of the reaction, the flow rate of O_2 is varied and the ratio of H_2 to O_2 was adjusted at 1.5, 2, 2.5, 3, 4 and 5. Each reaction experiment was performed at 200 °C and maintained up to 9 h. Between the reaction experiments, the reactor was kept at the reaction temperature with flowing inert gas, i.e. He or N_2, to both sides of the Pd membrane to prevent it from being damaged by any thermal impact.

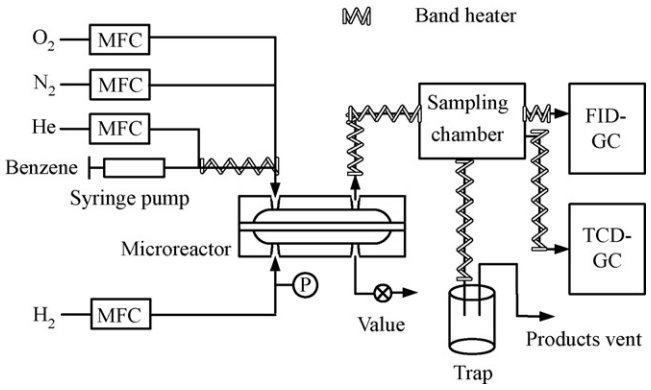

Fig. 4. Experimental setup for direct hydroxylation of benzene to phenol using MEMS-based PdMMR.

The reaction products of a fixed quantity of 0.5 ml were collected by a sampling chamber every hour during reaction and were introduced into two online gas chromatography systems; one was equipped with a thermal conductivity detector (TCD-GC) and the other one with a flame ionization detector (FID-GC). The inorganic gases were analyzed using the TCD-GC with a porous polymer column. The organic products of the reaction were analyzed using the FID-GC with a HP-70 capillary column (Hewlett-Packard, 30 m). The trapped products were identified by using a GC–MS (GC6890N with MSD9573, Agilent Technologies, Inc., not shown in Fig. 4).

We evaluated the H_2 permeation characteristics through the Pd membrane prior to the benzene hydroxylation experiments. The experimental setup is similar to that in Fig. 4, but mixture gases are replaced by pure N_2, which sweeps out the permeated H_2. H_2 flux through the Pd membrane was determined by measuring H_2 concentration in the N_2 stream with the TCD-GC.

He and N_2 permeation were also measured. He flux through the Pd membrane was determined by the same method with the H_2 flux. For the N_2 flux, a similar method was used except that sweep gas of pure He took place of pure N_2 on the upper side of the microreactor. After each change of the temperature and gas, the PdMMR was stabilized for at least 1 h.

4. Results and discussion

4.1. H_2 permeability and permselectivity of Pd membrane

The diffusion of H_2 through Pd membranes can be expressed in terms of Fick's first law

$$J = k(P_H^n - P_L^n), \quad (1)$$

where J is the H_2 flux, k is the diffusion constant depending on the thickness and temperature of the membrane, P_H and P_L are H_2 pressure at the inlet and H_2 partial pressure at the outlet, respectively, and n is the H_2 pressure exponent. It is reported that n is determined by the mechanism of H_2 permeation through the membrane [31]. $n = 0.5$ suggests that bulk diffusion is the rate controlling step of H_2 permeation. When the adsorption and desorption of H_2 on the membrane surfaces become more significant than bulk diffusion, n approaches 1. It has been claimed that surface processes control the permeation of very thin Pd films (submicron thickness) [32], and values of n close to 1.0 have been reported by several groups for very thin Pd films [32–34].

We prepared two PdMMRs under the same conditions of microfabrication. Also both Pd membranes have the same thickness of 500 nm by using the same sputtering time at the temperature of 200 °C. Fig. 5 shows H_2 flux through the Pd membrane of sample #1 as a function of H_2 partial pressure difference. This figure gives a

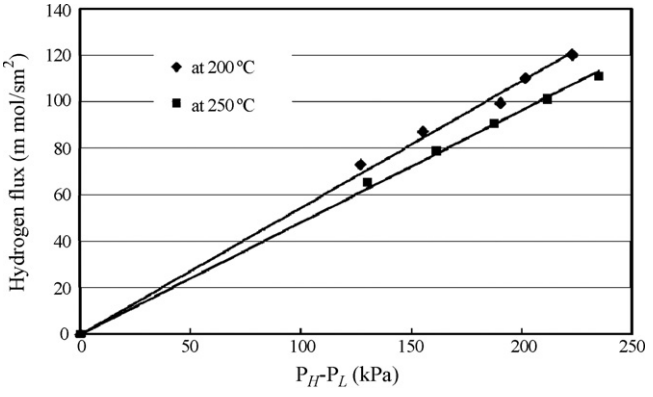

Fig. 5. Dependence of hydrogen flux through Pd membrane of sample #1 on the partial pressure difference of hydrogen.

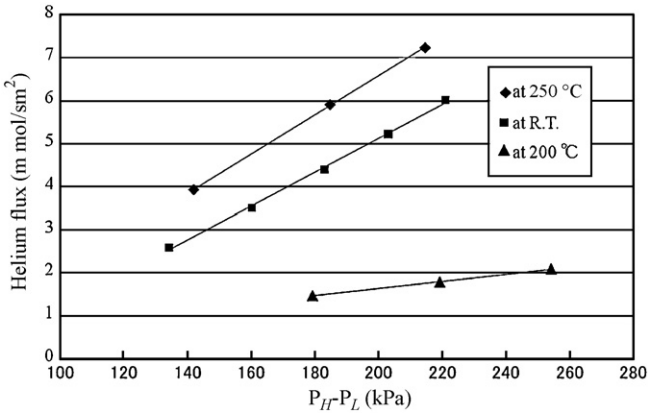

Fig. 6. Dependence of helium flux through Pd membrane of sample #1 on the partial pressure difference of helium.

linear dependence of the H_2 flux on the partial pressure difference of the H_2 on both sides of the membrane. The value of n close to 1.0 obtained here indicated that surface process dominated the H_2 permeation through the Pd membrane with submicron thickness. This result is also in consistency with our previous results [20].

The obtained H_2 permeation was 0.545 m mol/s m^2 kPa at a membrane temperature of 200 °C. The H_2 permeation through the Pd membrane should increase substantially with increasing temperature, but we did not observe higher H_2 permeation as expected when the temperature was increased from 200 °C to 250 °C. This phenomenon seems to be related to Pd oxidation. Pd oxidation can occur above 200 °C and reach the maximum of oxidation rate at about 300 °C [35]. To evaluate the permselectivity of the Pd membrane, we measured He and N_2 permeation through the Pd membrane. Table 1 shows the measurement sequence of gas permeation, gas permeation and corresponding permselectivity for sample #1. Note that the measurement of N_2 permeation (sequences 5 and 6) was carried out between the measuring steps of H_2 permeation at 200 °C and 250 °C (sequences 4 and 7), respectively. During the N_2 permeation tests, the Pd membrane may be oxidized to form palladium oxide by O_2, which is impurity existing in N_2. Pd oxidation resulted in both decrease in pinhole numbers, i.e. decrease in Knudsen flow, and decrease in atom hydrogen diffusion. Consequently, the H_2 permeation at 250 °C, which was measured after the N_2 permeation tests (sequences 5 and 6), might be lower than that at 200 °C.

Fig. 6 shows the dependence of He flux on the He partial pressure difference. As shown in Table 1, He permeation was measured at room temperature, 200 °C and 250 °C in the sequences 2, 3 and 8, respectively. A considerable decrease in He flux through the Pd membrane was observed when the temperature of the Pd membrane was raised from room temperature to 200 °C. This is attributed to decrease in pinhole numbers due to a larger thermal expansion coefficient of Pd than that of the oxidized PS support. We also found out that the He flux at 250 °C is considerably higher than that at 200 °C. As found in Table 1, the He flux at 250 °C was measured at sequence 8 directly after measuring H_2 permeation at 250 °C (sequence 7). It is well known that hydrogen embrittlement occurs when a Pd membrane contacts with H_2 at a temperature below 300 °C. Hydrogen embrittlement tends to cause lattice expansion in palladium, eventually cause it to delaminate. On the other hand, it was reported that a Pd membrane tightly packed in the pores of a support was resistant to hydrogen embrittlement [36]. In the PdMMR, the smooth and clean surface of the PS support might gave good gas tightness at 200 °C, but when temperature was raised from 200 °C to 250 °C, the delamination of the Pd membrane might occur due to the hydrogen embrittlement. This might result

Table 1
Measuring sequence of gas permeation, gas permeation and permselectivity of hydrogen for sample #1.

Measuring sequence	1	2	3	4	5	6	7	8
Measuring content	J_{N_2} @R.T.	J_{He} @R.T.	J_{He} @200 °C	J_{H_2} @200 °C	J_{N_2} @200 °C	J_{N_2} @250 °C	J_{H_2} @250 °C	J_{He} @250 °C
Gas permeation (m mol/s m^2 kPa)	0.0204	0.0393	0.008	0.545	0.0114	0.0097	0.482	0.046
Permselectivity of hydrogen			$J_{H_2,Seq.4}/J_{He,Seq.3} = 68.13$		$J_{H_2,Seq.4}/J_{N_2,Seq.5} = 47.81$	$J_{H_2,Seq.7}/J_{N_2,Seq.6} = 49.73$		$J_{H_2,Seq.7}/J_{He,Seq.8} = 10.49$

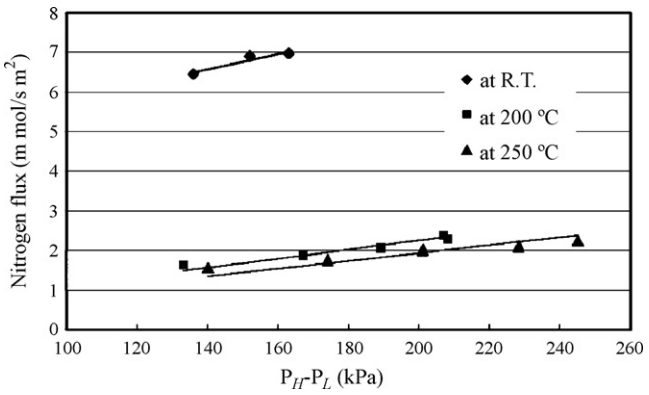

Fig. 7. Dependence of nitrogen flux through Pd membrane of sample #1 on the partial pressure difference of nitrogen.

in large increase in pinhole numbers and eventually increase in Knudsen flow. The permselectivity of H_2 to He at 200 °C and 250 °C are 68.13 and 10.49, respectively, as shown in Table 1. For single gas permeation test, the sequence of the gas permeation affects importantly the results of permselectivity [35]. The real permselectivity of H_2 to inert gas, e.g. He or N_2, should be defined as the ratio of H_2 permeation to inert gas permeation measured directly after the H_2 permeation test [35], taking account of the above Pd delamination effect. Therefore, a value of 10.49 represents a real permselectivity of H_2 to He at 250 °C in our test.

Fig. 7 shows the dependence of N_2 flux on the N_2 partial pressure difference. In Fig. 7, we also observed considerable decrease in N_2 flux through the Pd membrane when the temperature of the Pd membrane was raised from room temperature to 200 °C, as observed for He flux. The N_2 flux showed small decrease when the temperature was raised from 200 °C to 250 °C. The permselectivity of H_2 to N_2 at 200 °C and 250 °C are 47.81 and 49.73, respectively. Note that the permeation of N_2 at 200 °C was measured directly after the H_2 permeation test, and thus the value at 200 °C can be reasonably compared with the permselectivity of H_2 to He at 250 °C.

Next, we evaluated another PdMMR (sample #2). The measurement sequence for sample #2 is shown in Table 2. To eliminate the possibility of Pd oxidation, we did not measure N_2 permeation for this sample. Figs. 8 and 9 give the dependence of He and H_2 flux on the partial pressure difference of He and H_2, respectively. We obtained the H_2 permselectivity of 36.79 to He at 250 °C. However, the permselectivity of H_2 to He at 200 °C is only 2.12, which is considerably smaller than that at 250 °C. It must be noted that He permeation at 200 °C was measured directly after H_2 reduction,

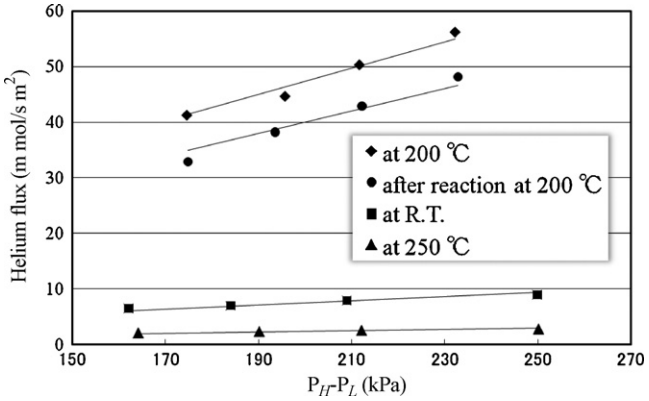

Fig. 8. Dependence of helium flux through Pd membrane of sample #2 on the partial pressure difference of helium. The data measured after benzene hydroxylation tests at 200 °C is also shown (labeled as "after reaction at 200 °C").

Table 2
Measurement sequence of gas permeation, gas permeation and permselectivity of hydrogen for sample #2.

Measuring sequence	1	2	3	4	5	6	7	8
Measuring content	J_{He} @R.T.	J_{He} @250 °C	J_{H_2} @250 °C	H_2 reduction @250 °C for 2 h	J_{He} @200 °C	J_{H_2} @200 °C	J_{H_2} @200 °C after reaction	J_{He} @200 °C after reaction
Gas permeation (m mol/s m² kPa)	0.0377	0.012	0.4415		0.2368	0.5016	0.2002	0.3955
Permselectivity of hydrogen		$J_{H_2,Seq.3}/J_{He,Seq.2} = 36.79$			$J_{H_2,Seq.3}/J_{He,Seq.5} = 2.12$			$J_{H_2,Seq.7}/J_{He,Seq.8} = 1.98$

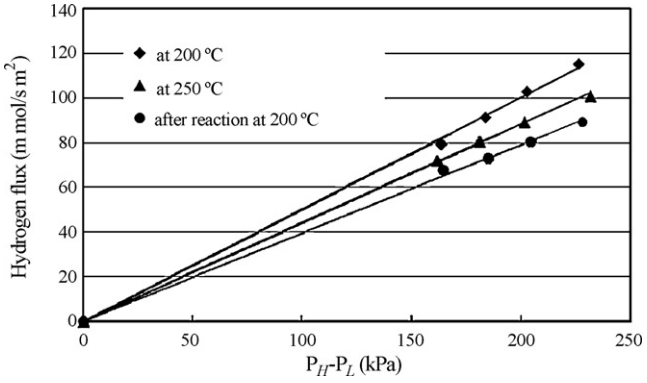

Fig. 9. Dependence of hydrogen flux through Pd membrane of sample #2 on the partial pressure difference of hydrogen. The data measured after benzene hydroxylation tests at 200 °C is also shown (labeled as "after reaction at 200 °C").

as shown in Table 2. The object of the H_2 reduction after the H_2 permeation test at 250 °C aimed to improve H_2 permeation, but it might result in critical hydrogen embrittlement. Due to hydrogen embrittlement, He permeation showed dramatic increase, and the permselectivity of H_2 to He at 200 °C decreased to 2.12. This value is still larger than the ideal Knudsen selectivity of H_2 to He (1.41) suggesting that atom hydrogen diffused still through the Pd membrane. From Fig. 9, we found out that the H_2 permeation at 250 °C was 0.4415 m mol/s m² kPa, but H_2 permeation at 200 °C was 0.5016 m mol/s m² kPa, which was higher than that at 250 °C. This might be also attributed to increase in Knudsen flow due to hydrogen embrittlement.

The permselectivity of two samples showed much difference. This is because of difference of hydrogen embirttlement in degree. Taking account of real permselectivity, the permeation and permselectivity of sample #1 is still comparable to our results reported previously [20].

The permselectivity of the PdMMRs obtained in this study is much lower than that of the PdMRs (typically 10E6 at 200–300 °C), which was prepared by CVD, reported by Sato et al. [16]. This might be attributed to the difference in the deposition mechanism between sputter-deposition and CVD. For sputter-deposition, metal atoms form loosely bonded atomic clusters, which are adhered on the surface of the porous support. Therefore, the Pd membrane has low resistant to hydrogen embrittlement, although a Pd membrane made by sputtering may be densified to a higher extent during high temperature test. While for CVD, since deposition is a surface reactive process, Pd precursor vapor can infiltrate inside the porous support, adsorbed on the pore surface, and react to form Pd, which tightly pack in the pores of the support. Therefore, the Pd membrane made by CVD shows good resistant to hydrogen embrittlement even below 300 °C due to mechanical containment effect [13–18,36].

4.2. Reaction of benzene hydroxylation

Fig. 10 shows the result of benzene hydroxylation at a H_2/O_2 ratio of 4 for sample #2. (Sample #1 broke before the benzene hydroxylation tests by accident, and there is no reaction data.) We can find that the yields of phenol and other products remain relatively constant during the reaction term up to 9 h. The yield of phenol is around 20% and the conversion of benzene is around 54%. Main by-products are CO_2, 2-hydroxycyclohexanone ($C_6H_{10}O_2$) and p-benzoquinone ($C_6H_4O_2$). Such a result, i.e. a high yield of phenol accompanying with a relatively high benzene conversion of 54% and a relatively high phenol selectivity of 37%, is different from that for the tubular PdMRs [13,14,16–18]. The highest yield of phenol for the tubular PdMRs was 15.1% in Ref. [13] and [16–18].

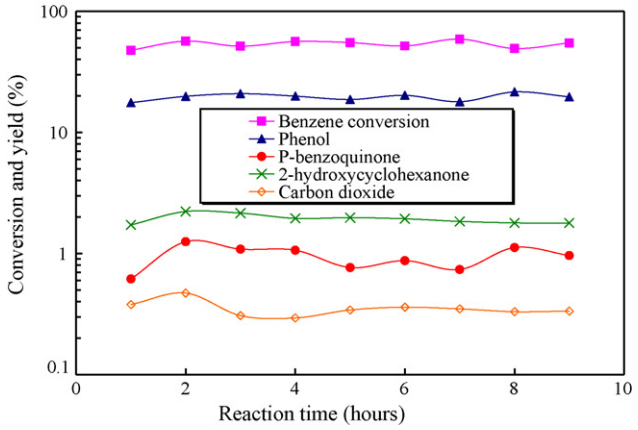

Fig. 10. Conversion and yield of each product during test term up to 9 h.

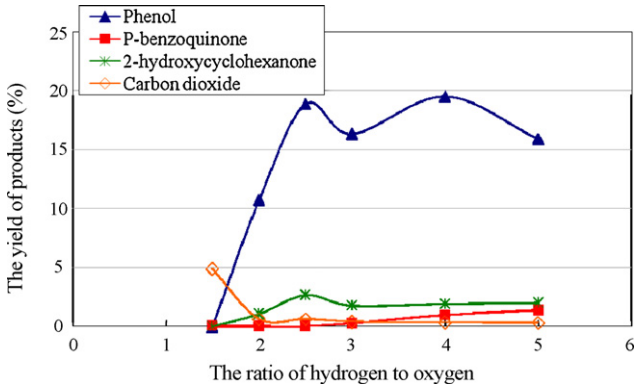

Fig. 12. The dependence of yields on the ratio of H_2/O_2 for the MEMS-based PdMMR.

Although a yield of 20–23% and a selectivity of 77% for phenol were reported in Ref. [14], the conversion of benzene was only within 25–30%.

The MEMS-based PdMMRs have a small dimension of 5 mm × 5 mm and a large surface-to-volume ratio of ca. 100, while the tubular PdMRs have a large dimension (100 mm in length) and a small surface-to-volume ratio of ca. 3. Large surface-to-volume can provide faster response to reaction. The permeated hydrogen species via the Pd membrane could react with oxygen and benzene immediately and such a fast reaction prevented the permeated hydrogen species from being recombined on the Pd membrane. Since active hydrogen species were used effectively for hydroxylation of benzene, a higher yield of phenol and a higher conversion of benzene were obtained.

An estimated reaction pathway is summarized in Fig. 11. Dihydroxy compounds from the phenol hydroxylation, 1, 2-benzenediol and hydroquinone ($C_6H_6O_2$), have a high reactivity so that they were hydrogenated or dehydrogenated, and formed main by-products of 2-hydroxycyclohexanone ($C_6H_{10}O_2$) and p-benzoquinone ($C_6H_4O_2$), respectively. Besides the above-mentioned main by-products, a very small amount of 1, 2-benzenediol, hydroquinone and 1, 4-cyclohexanedione were also detected by the GC–MS. We also observed water formation using the GC–TCD with the polymer porous column.

We investigated the effect of H_2/O_2 ratio on benzene hydroxylation. Fig. 12 shows the dependence of the product yields on the ratio of H_2/O_2. For all experiments of benzene hydroxylation, H_2 permeated flux was kept at 1.5 cc/min by controlling the pressure of H_2 in the inlet. We just adjusted the flux of O_2 to change the ratio of H_2/O_2. When $H_2/O_2 < 1.5$, only CO_2 was identified. Hydroxylation cannot occur with an over amount of oxygen, although H_2 permeated through the Pd membrane. This suggests that the atmosphere on the Pd membrane was almost controlled by oxygen and only oxidation is a possible reaction. When $H_2/O_2 > 1.5$, the hydroxylation reaction occurred and developed with decrease in oxygen concentration. Naturally, oxidation showed decreasing trend with decrease in oxygen concentration. This can be supported by increase in phenol yield and decrease in carbon dioxide yield in Fig. 12 till $H_2/O_2 = 2.5$. When $H_2/O_2 > 2.5$, phenol yield showed an almost stable value of around 20%. Simultaneously, carbon dioxide yield was also kept the lowest value close to zero level.

It is worthwhile to compare our results of benzene hydroxylation with those of the tubular PdMRs [13–18]. First, the transformation of dominating reaction from oxidation to hydroxylation of the benzene in our case occurred at a lower ratio of H_2/O_2 than that in tubular PdMRs [15,17]. The yield of carbon dioxide became almost zero when the ratio of H_2/O_2 was increased to 2.5 in the PdMMR, while the corresponding ratio of H_2/O_2 in the tubular PdMRs was above 7 at the very least [15,17] as shown in Fig. 13, which was reproduced from Ref. [17].

Second, the yield of phenol was kept at around 20% stably when the ratio of H_2/O_2 was changed above 2.5 in our experiment. For the tubular PdMRs, there was an optimum H_2/O_2 ratio (4–4.6) giving the largest phenol yield, as shown in Fig. 13 [14,17]. Benzene has three kind of reaction trend, which are hydroxylation, oxi-

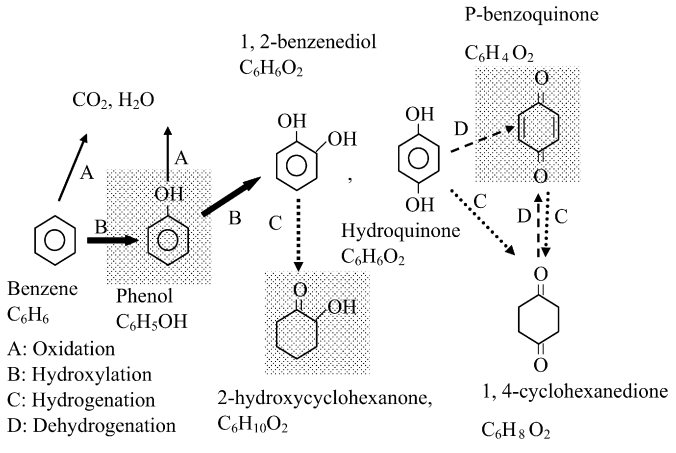

Fig. 11. Estimated reaction pathways for benzene hydroxylation. The compounds boxed by meshes are main product (phenol) and main by-products. Other by-products exist in a very small amount.

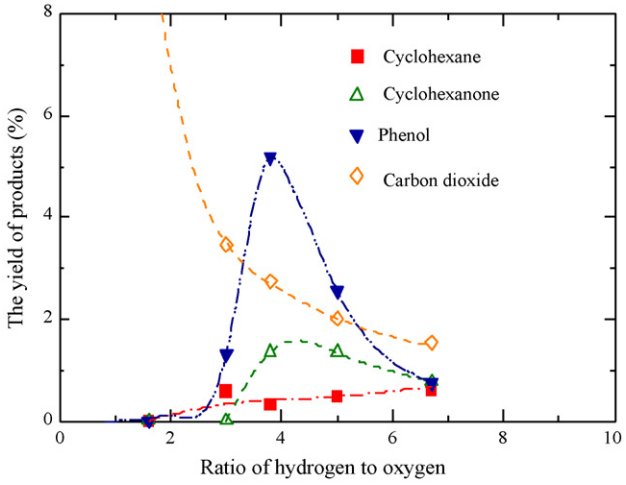

Fig. 13. The dependence of yields on the ratio of H_2/O_2 for the tubular PdMR. The graph is reproduced from Ref. [17].

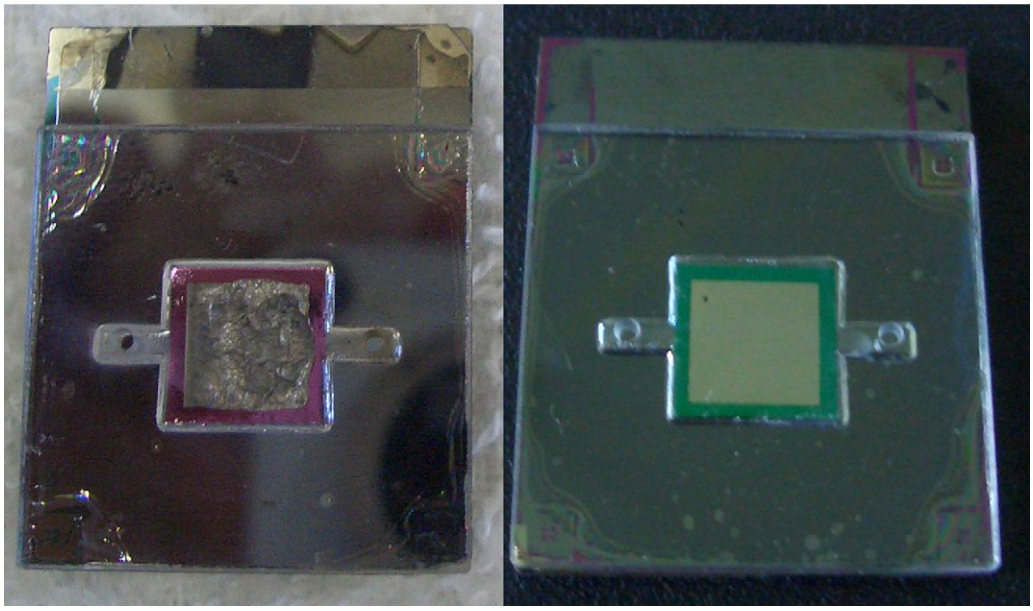

Fig. 14. The comparison between the surfaces of the used (left) and unused (right) Pd membrane. The samples are not the same one.

dation and hydrogenation, on the Pd membrane covered by the mix gas of oxygen and H_2. In the macrotubular PdMRs, oxidation and hydrogenation regions existed on the same Pd membrane and hydroxylation occurred only in the limited region [15]. When the ratio of H_2/O_2 was adjusted, oxidation and hydrogenation became strong or weak correspondingly. As a result of competition between oxidation and hydrogenation, hydroxylation shows the highest yield at the optimum ratio of H_2/O_2.

On the contrary, since the PdMMRs have a micro-dimension, the distribution of the reactant gas concentration could be almost uniform on the surface of the Pd membrane. When oxygen concentration was decreased to some level (in our case, H_2/O_2 is 2.5), the active hydrogen species covered uniformly over the surface of the Pd membrane. Due to a large surface-to-volume ratio, they have a high probability to meet and react with molecules of oxygen and produced fast active oxygen species on the whole surface of the Pd membrane. Correspondingly, these active oxygen species also reacted fast with benzene. As a result, hydroxylation could dominate quickly over the whole surface of the Pd membrane and special reaction regions might not be formed as reported in Refs. [13–18], even when H_2/O_2 ratio was changed. Small dimension and large ratio of surface-to-volume were the reason for the PdMMR achieving the largest the yield of phenol at a lower ratio of H_2/O_2 (2.5) than that (4–4.6) in the PdMRs, and for transformation of dominating reaction from oxidation to hydroxylation of the benzene at a lower ration of H_2/O_2 in the PdMMR.

Third, the distribution of products in the PdMMR is very different form that in the PdMRs. As shown in Figs. 11 and 12, the phenol, dihydric phenols such as 1, 2-benzenediol and hydroquinone ($C_6H_6O_2$), and the products from the dihydric phenols dominated the distribution of products. The hydrogenation products of cyclohexane (C_6H_{12}) and cyclohexanone ($C_6H_{10}O$) from benzene and phenol were not detected, even when the ratio of H_2/O_2 was adjusted up to 5. While in Refs. [13–18], the hydrogenation products from the benzene and phenol were main by-products. Under the condition of abundant hydrogen, some hydrogen atoms permeated via a Pd membrane recombined into hydrogen molecules out of the surface of the Pd membrane. These hydrogen molecules could be swept out from the PdMMRs quickly due to a small dimension of reactors, before they could react with benzene and other products. This might be one reason of the absence of hydrogenation products from the benzene and phenol. The absence of hydrogenation from benzene and phenol also contributed to a higher yield of phenol.

Phenol yield of 20% in the PdMMR is comparable to the yield of 20–23% in Ref. [14]. High phenol yield accompanying with high benzene conversion of 54% is benefit from the miniaturization of Pd membrane reactors. While in Ref. [14], high phenol yield was accompanied with high phenol selectivity of 77%. This is reasonable result because there is a trade-off between the benzene conversion and phenol selectivity. It is noted that the products were dominated by phenol and dihydric phenols in the PdMMR. It is expected that high yield accompanying high conversion and selectivity could be obtained if reaction conditions are adjusted adequately.

Figs. 8 and 9 also give the permeation of He and H_2 for sample #2 after finishing all of test experiments. The total reaction time was around 200 h, and the total time of permeation measurement was around 50 h. The H_2 permeation showed a decrease of about 21% and that of He showed a decrease of about 16% after all of reaction experiments. The permselectivity of H_2 to He after all experiments was decreased to 1.98, which is a little lower than that (2.12) before the experiments. The decrease of gas permeation should be attributed to carbon pollution during hydroxylation of benzene. Fig. 14 shows the comparison between the surfaces of the used and unused Pd membrane. The samples are not the same one. We can observe that the used surface lost its metallic luster compared to the unused surface, and became black. This supports that the surface of the Pd membrane was polluted by carbon material existing in reactants. We also observed peeling of the Pd membrane due to hydrogen embrittlement. This means the stability of the Pd membrane is still a challenge for long reaction. It was reported that the Pd membrane made by CVD [13–18,36] have good resistant to hydrogen embrittlement. Therefore, it is possible to improve the stability of the Pd membrane by using a Pd membrane made by CVD or a Pd–Ag membrane in the PdMMRs instead of the Pd membrane made by sputtering.

5. Conclusions

We carried out one-step conversion of benzene to phenol using novel MEMS-based PdMMRs, in which a 500-nm thick Pd membrane was supported by a porous silicon layer. We also evaluated

the H_2 permeation characteristics through the Pd membrane before the benzene hydroxylation experiments. At 200 °C, the H_2 permeation is 0.545 m mol/s m^2 kPa and the permselectivity of H_2 to N_2 is 47.8. These values are comparable to that reported previously [20], but these values were still lower than that of a Pd membrane made by CVD. This might be attributed to the difference in the deposition mechanism between sputtering and CVD.

The phenol yield of 20% and benzene conversion of 54% were obtained at a reaction temperature of 200 °C. This result is better than that in the macrotubular PdMRs. The effect of H_2/O_2 ratio on products distribution has been investigated. The results have been compared with those of a macrotubular PdMRs. Since the PdMMRs had a smaller dimension and a larger ratio of surface-to-volume comparing to PdMRs, active hydrogen species were used more effectively for hydroxylation of benzene on the Pd surface of the PdMMRs. Therefore, the PdMMRs can finish transformation of dominating reaction from oxidation to hydroxylation of the benzene and achieve the largest the yield of phenol at lower ratio of H_2/O_2. Due to active hydrogen species were used more effectively, a higher yield of phenol accompanying a higher conversion of benzene was obtained. Also, the products distribution in the PdMMRs was very different from the PdMRs. Phenol and dihydric phenols dominated products distribution in PdMMR, and the hydrogenation products of cyclohexane (C_6H_{12}) and cyclohexanone ($C_6H_{10}O$) from benzene and phenol were not detected in the PdMMR, while the hydrogenation products from benzene and phenol were main by-products in the PdMRs.

The stability of the Pd membrane is still a challenge for long reaction. However, it is possible to improve the stability of the Pd membrane by using a Pd membrane made by CVD or a Pd–Ag membrane instead of the Pd membrane made by sputtering in the PdMMRs.

Acknowledgments

The authors would like to thank Dr. T. Hanaoka from National Institute of Advanced Industrial Science and Technology (AIST) for his kind help in reaction experiments.

References

[1] M. Iwamoto, J. Hirata, K. Matsukami, S. Kagawa, J. Phys. Chem. 87 (1983) 903–905.
[2] E. Suzuki, K. Nakashiro, Y. Ono, Chem. Lett. 17 (1988) 953–956.
[3] G.I. Panov, V.I. Sobelev, A.S. Kharitonov, J. Mol. Catal. 61 (1990) 85–97.
[4] L.V. Pirutko, V.S. Chernyavsky, A.K. Uriarte, G.I. Panov, Appl. Catal. A: Gen. 227 (2002) 143–157.
[5] S.K. Das, A. Kumar Jr., S. Nandrajog, A. Kumar, Tetrahedron Lett. 36 (1995) 7909–7912.
[6] W. Zhang, J. Wang, T. Tanev, T.J. Pinnavaia, Chem. Commun. (1996) 979–980.
[7] K. Nomiya, H. Yanagibayashi, C. Nozaki, K. Kondoh, E. Hiramatsu, Y. Shimizu, J. Mol. Catal. A: Chem. 114 (1996) 181–190.
[8] D. Bianchi, R. Bortolo, R. Tassinari, M. Ricci, R. Vignola, Angew. Chem. Int. Ed. 39 (2000) 4321–4323.
[9] T. Jintoku, H. Taniguchi, Y. Fujiwara, Chem. Lett. 16 (1987) 1865–1868.
[10] A. Kunai, T. Wani, Y. Uehara, F. Iwasaki, Y. Kuroda, S. Itoh, K. Sasaki, Bull. Chem. Soc. Jpn. 62 (1989) 2613–2617.
[11] T. Tatsumi, K. Yuasa, H. Tominaga, J. Chem. Soc. Chem. Commun. (1992) 1446–1447.
[12] H. Ehrich, H. Berndt, M.-M. Pohl, K. Jahnisch, M. Baerns, Appl. Catal. A: Gen. 230 (2002) 271–280.
[13] S. Niwa, M. Eswaramoorthy, J. Nair, A. Raj, N. Itoh, H. Shoji, T. Namba, F. Mizukami, Science 295 (2002) 105–107.
[14] N. Itoh, S. Niwa, F. Mizukami, T. Inoue, A. Igarashi, T. Namba, Catal. Commun. 4 (2003) 243–246.
[15] K. Sato, S. Niwa, T. Hanaoka, K. Komura, T. Namba, F. Mizukami, Catal. Lett. 96 (2004) 107–112.
[16] K. Sato, T. Hanaoka, S. Niwa, C. Stefan, T. Namba, F. Mizukami, Catal. Today 104 (2005) 260–266.
[17] K. Sato, T. Hanaoka, S. Hamakawa, F. Mizukami, Proceeding of 5th World Congress on Oxidation Catalysis, September, Sapporo, Japan, 2005, pp. 238–239.
[18] K. Sato, T. Hanaoka, S. Hamakawa, M. Nishioka, K. Kobayashi, T. Inoue, T. Namba, F. Mizukami, Catal. Today 118 (2006) 57–62.
[19] R. Srinivasan, I.M. Hsing, P.E. Berger, K.F. Jensen, AIChE J. 43 (1997) 3059–3069.
[20] S.-Y. Ye, S. Tanaka, M. Esashi, S. Hamakawa, T. Hanaoka, F. Mizukami, J. Micromech. Microeng. 15 (2005) 2011–2018.
[21] S.M. Lai, C.P. Ng, R. Martin-Aranda, K.L. Yeung, Microporous Mesoporous Mater. 66 (2003) 239–252.
[22] S.M. Lai, R. Martin-Aranda, K.L. Yeung, Chem. Commun. 2 (2003) 218–219.
[23] X.F. Zhang, S.M. Lai, R. Martin-Aranda, K.L. Yeung, Appl. Catal. A. 261 (2004) 109–118.
[24] W.N. Lau, K.L. Yeung, R. Martin-Aranda, Microporous Mesoporous Mater. 115 (2008) 156–163.
[25] Y.S.S. Wan, K.L. Yeung, A. Gavriilidis, Appl. Catal. A. 281 (2005) 285–293.
[26] Y.S. Cheng, M.A. Pena, K.L. Yeung, J. Taiwan Inst. Chem. Eng. 40 (2009) 281–288.
[27] J.L.H. Chau, A.Y.L. Leung, K.L. Yeung, Lab-on-a-Chip 3 (2003), 53.
[28] A.Y.L. Leung, K.L. Yeung, Chem. Eng. Sci. 59 (2004), 4809.
[29] Y. Moro-oka, M. Akita, Catal. Today 41 (1998) 327–338.
[30] K. Otsuka, I. yamanaka, H. Hosokawa, Nature 345 (1990) 697–698.
[31] R. Dittmeyer, V. Höllein, K. Daub, J. Mol. Catal. A: Chem. 173 (2001) 135–184.
[32] V. Jayaraman, Y.S. Lin, J. Mem. Sci. 104 (1995) 251–262.
[33] S.-E. Nam, S.-H. Lee, K.-H. Lee, J. Mem. Sci. 153 (1999) 163–173.
[34] L.Q. Wu, N. Xu, J. Shi, AIChE J. 46 (2000) 1075–1083.
[35] D.-W. Lee, Y.-G. Lee, S.-E. Nam, S.-K. Ihm, K.-H. Lee, J. Mem. Sci. 220 (2003) 137–153.
[36] S. Yan, H. Maeda, K. Kusakabe, S. Morooka, Ind. Eng. Chem. Res. 33 (1994) 616–622.